AIAA-2005-1620
(With corrections)

Inflation and Steady-Descent Characteristics of Truncated Cone Decelerators

By

Jean Potvin [Э]
Saint Louis University, St. Louis, MO 63103, USA

and

Gary E. Peek [Ж]
Industrologic Inc., St. Charles, MO 63301, USA

We report on the results of a "first look" study of the inflation and descent characteristics of a new type of parachute – the truncated cone decelerator (or "TCD"). Featuring a deep conical inflated shape truncated at the apex, the TCD is being envisaged for use in wind-sensing applications where GPS-instrumented payloads are to be drifting freely with the wind, in a stable manner and without gliding. The combination of a low axial drag area with a high transverse drag area should rank the TCD as one of the best performers for this type of applications. The paper first presents the design characteristics of the two 2.3 height-to-base -ratio cones that were used in this study, namely a three foot-long model and a 16ft-long model. Next comes the discussion of the experimental data on fall rates, which yielded drag coefficient values approximating $C_D \sim 0.25$. Data was also obtained with the sub-scale model being truncated at the vent, at lengths ranging from 0% to 20% of the original cone height. The paper ends with a discussion of the inflation properties, which yielded low peak drag forces and non-dimensional filling time values approximating $n_{fill} \sim 13$ to 20.

Nomenclature

B = base length of the triangular pattern used to build a TCD
C_D = drag coefficient during the steady state descent
d = diameter of the inflated conical shape
C_k = opening shock factor
F_{max} = maximum drag generated during inflation
H = height of the triangular pattern used to build a TCD
n_{fill} = non-dimensional filling time
R_m = mass ratio
$SC_D|_{steady}$ = steady state drag area
S_P = projected surface area
S_T = total cone surface area (without apex vent)
S_{TF} = total fabric surface area
S_V = apex vent surface area
t_{fill} = (dimensional) filling time
$V_{stretch}$ = speed of the parachute-payload system at line stretch
VHT = height of the cone outlining the fabric that was removed to make an apex vent
W = total weight of the system

[Э] Department of Physics, 3450 Lindell Blvd, St. Louis, MO 63103, member AIAA
[Ж] 3201 Highgate Lane, St. Charles, MO 63301

(Corrected, 5 February, 2011)

1. Introduction

Truncated cones have been around aviation for a great many years, having been used mostly as wind gauges in the form of the ubiquitous airport wind sock (figure 1.1). Lately, slightly tapered cones have made their appearance in the sport of skydiving to enhance the fun of freefall during so-called "freeflying" dives (figure 1.2). Deep cone-like shapes used with their skirt opened to the incoming wind, like the one example shown in figure 1.3, have never been used as decelerators or stabilizing devices except perhaps for DaVinci's well-known pyramidal parachute. The reason for this is simple: because of their lack of bluffness, or in other words of their extreme rearward streamlining, deep cones are characterized by small values of the drag coefficient - typically a third of those of hemispherical parachutes or of standard "conical" parachutes (which are shallow cones). From the point of view of drag production per unit fabric weight, deep cones are quite inefficient at generating drag and therefore must be used at much larger sizes to generate the same drag force that smaller hemispherical parachutes would usually produce. In applications where weight and packing volume are at a premium, such inefficiency is all that is needed to discard deep cones from further design consideration.

Recently, GPS-equipped parachute-payload systems freely drifting with the wind have been used for the real-time measurement of the wind column over a drop zone.[1-4] High porosity parachutes are used for that purpose because of their stability and non-gliding properties, which are important requirements for this type of application. But deep cones can do the job as well. In fact, they can do an even better job at wind-drifting given the larger surface area "footprint" that is projected along the horizontal. Such a large "transverse" drag area footprint (with respect to the direction of fall) causes cones to adjust to wind changes more quickly than standard hemispherical chutes of similar longitudinal drag area. And so, the very design characteristic that causes conical parachutes to be inefficient decelerators makes them quite efficient at being wind drifters.

The paper reports on the results of a "first look" study of the basic inflation and descent characteristics of one type of deep cone parachute, namely the so-called truncated cone decelerator (or "TCD"), which is a cone truncated at the apex. First, the design characteristics and sizes of the cones that were used in this study are discussed. New experimental data on fall rates and inflation characteristics are then presented.

Figure 1.1 The common airport wind sock.

Figure 1.2 Slightly tapered tubes used in "freestyle" skydiving.

Figure 1.3 One example TCD used in this study. Note that the the cruciform parachute shown next to the TCD features the same drag area. Note also that the TCD shown has four suspension lines.

2. Design Characteristics

The TCDs used in this study featured only one basic *cone* aspect ratio, namely one of height-to-inflated base ratio of about 2.3 to 2.4. This value was motivated mainly by the desire of using a cone that was different in shape from that of a near hemisphere, which can be seen as a "cone" of aspect ratio smaller than unity. There was also the desire of avoiding the use of straight tubes which are cones of infinite aspect ratio.

The cone aspect ratio used here is based on the basic triangular gore pattern shown in figures 2.1 and 2.2. Mathematically, the cone's aspect ratio is expressed in terms of the gore's vertical height over the cone's inflated

base diameter, or *H/d*. In a two-gore design $H/d = \pi H/2B$. The study involved the use of two basic sizes of the same aspect ratio, here denoted as "sub-scale" and "full-scale" respectively:

- Sub-scale: *B = 41.0in* and *H = 63.0in; variable VHT*;
  total parachute-payload weight = 4.1 lb. H/d = 2.41.

- Full-scale: *B =10.66ft and H = 16.0ft*; *VHT = 26.7in*; *VHT/H* = 13%;
  total parachute-payload weight = 18.0 lb. H/d = 2.35.

The small-scale TCD was built out of two gores made of standard F-111 fabric cut into the pattern of opposed double-isosceles triangles shown in figure 2.2. The *gore* aspect ratio of these pieces was H/B = 3/2. The shallow inverted isosceles triangular extension on each gore made was added to insure the same tension on each of the four equal-length suspension lines used with this design. The large-scale model, on the other hand, involved eight suspension lines of equal length, thus necessitating the use of four gores cut as right triangle (plus extensions). Pairs of these triangles yielded the same basic shape of figure 2.1 with a *gore aspect ratio* of about $H/B \sim 3/2$. At both scales the TCDs were outfitted with suspension lines of length equal to the cone base (while laying flat). Such combinations yielded an inflated shape that is truly a cone of revolution, in contrast with the use of only one isosceles triangle (per gore) and four equal length suspension lines, which resulted in an inflated cone with an "oval" skirt. Note that in the case of the sub-scale TCD, the diameter of the apex vent was changed in small increments and re-dropped as further discussed below. The surface areas of relevance to this design are as follows (again with reference to figures 2.1 and 2.2):

- Total cone surface area (2 gores; without apex vent; neglecting the shallow inverted isosceles triangle): $S_T = 2\,(B/2)\,H = BH$
- Apex vent surface area: $S_V = (B^2/\pi)(VHT/H)^2$
- Total fabric surface area: $S_{TF} = S_T - S_V$
- Area of the surface outlined by the inflated skirt (defines also the projected diameter): $S_P = B^2/\pi$

The area S_T will be considered as the *nominal area* of the cone for the purpose of drag coefficient calculation with or without the use of an apex vent.

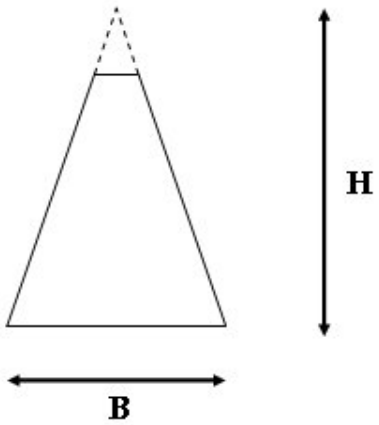

ASPECT RATIO = H/B

Figure 2.1 Definition of the basic TCD *gore* aspect ratio. In its simplest rendition, a TCD can be built out of two fabric pieces cut as isosceles triangles. The figure shows one such piece as laid on a flat surface.

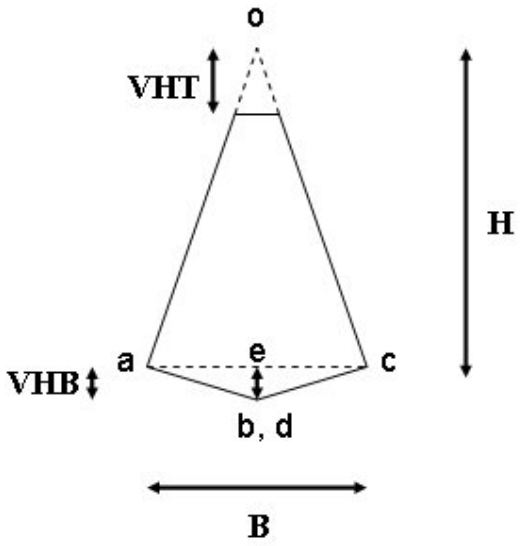

$$VHB = eb = ed = oa - oe = ((B/2)^2 + (H)^2)^{0.5} - (H)$$

Figure 2.2 Fabric template for the sub-scale TCDs. Note the opposed double-isosceles triangle configuration of the two gores. Points *a, b, c* and *d* mark the locations of the suspension line attachment points for the sub-scale example.

Figure 2.3 Photo of the 16ft-tall TCD that was drop-tested during the inflation study. Photo courtesy of the St. Louis Post Dispatch – reprinted with permission.

3. Fall Rates and Inflation Characteristics

3.1 Experimental conditions

The fall rates of both small- and large-scale TCD's were obtained using payloads instrumented with an Industrologic VSI pressure sensor, which measured the AGL-altitude during inflation and during the steady state portion of the descent. An Industrologic PDAS data acquisition unit was used to record this data, at a rate of 10 Hz in the case of the half-scale parachutes, and at a rate of 1000 HZ in the case of the full-scale parachute. See figures 3.1 and 3.2 below. The high frequency used in the full-scale parachute tests was required by the inflation study that took place during the same drops, a study that involved the measurement of the loads sustained by the risers. These measured loads involved the use of home-made load cells of the type shown in figure 3.3; such data was piped to the same PDAS data acquisition unit used by the VSI sensor.

The payload container used with the full-scale parachute was a weighted plastic milk crate of dimensions 12"x12"x13", and with a built-in under-shelf holding a 15-lbs dumbbell weight. Including instrumentation and parachute hardware, the total weight of the system was set at 18 lbs in order to yield descent rates characteristic of ongoing parachute gliding studies[3]. The parachutes and container were linked by an "H"-type riser with 23" separation (see figures 2.3 or 3.7). In the case of the half-scale drops the payload container consisted of a light-weight bag enclosing the VSI and PDAS units, resulting in a total parachute-payload weight of 4.1lbs.

Because of the associated small light weights and sizes, all drops of the sub-scale TCDs were performed by a parachutist flying under his own parafoil canopy, typically at a height of 1000 – 2000 ft AGL, and over the grounds of the Vandalia Municipal Airport in Vandalia, IL (field elevation of 538 ft MSL). Table 3.1 shows the fall rate data that was measured. On the other hand, all full-scale parachute drops where carried out from a Cessna Caravan aircraft and from heights of 500 to 800 ft AGL, also in Vandalia, IL. These drops took place in October and November of 2004. The parachute-payload bundle was dropped from the aircraft side-door at 120 mph (indicated) and the parachute was deployed with a direct-bag static line system. Video of the deployment and inflation sequence was taken from the aircraft; video of the deployment, inflation sequence *and* steady-state descent was taken from the ground also. The measured riser loads and fall rates are shown in figures 3.4 – 3.6. Figure 3.7 shows the inflation sequence that occurred during drop YPG034.

Figure 3.1 VSI rate-of-descent sensor.

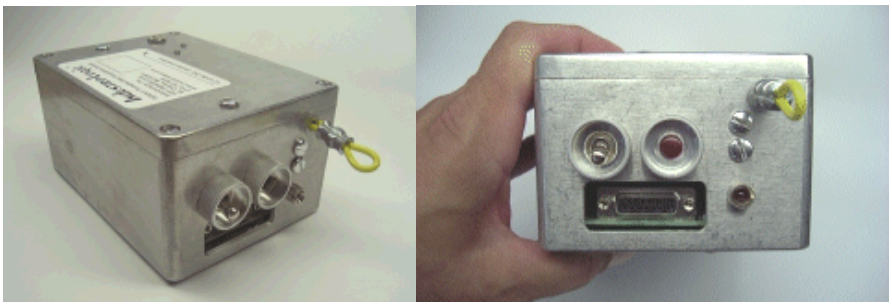

Figure 3.2 Two views of the Industrologic "PDAS" data acquisition unit used in this experimental study.

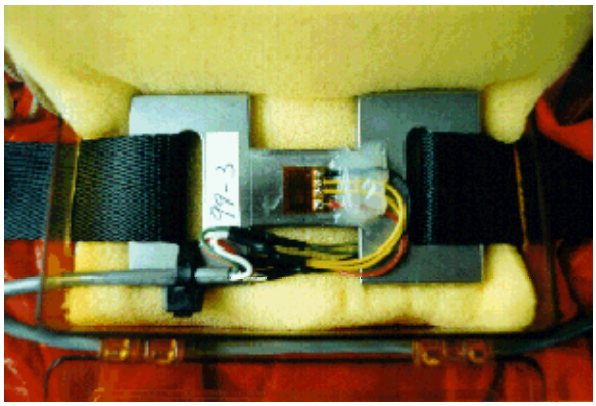

Figure 3.3 Pictures of the home-made riser load link.

3.2 Fall rates and drag coefficient

The steady state fall rates of the half-scale parachutes are shown in Table 3.1 below. With a total weight of 4.1lb, these yielded a range of 29 to 33 ft/sec. Compared to the "no-vent" configuration, this fall rate appears to *decrease* with *increasing* vent size. However, this phenomenon may be a small-vent effect, and is followed by the fall rate increasing with vent area as generally expected. The values of the nominal drag coefficient C_{D0} (i.e., computed with S_T as reference area) shows the same trend but in the opposite direction, with a mean of $C_{D0}^{mean} \sim 0.23$. So it appears that there is a range of vent size where the vent outflow actually contributes to the reduction of the mean pressure in the near-wake.

The fall rates measured with the full-scale system are shown in figures 3.4 - 3.6. Excluding the strange data of YPG040 which was due to unusual meteorological conditions near the ground, the fall rate averaged over the entire post-inflation descent ended up at 17.2 and 20.1 ft/sec, yielding drag coefficient values of C_{D0} = 0.30 and 0.23 respectively. Note that VHT/H = 0.14 for the full-scale parachute, and that its drag coefficient value is consistent with that of the sub-scale parachute of similar ratio, namely VHT/H = 0.12 and C_{D0} = 0.26.

Note that several non-instrumented test drops of sub-scale TDCs have shown that very large apex vents sizes –namely of order $S_V/S_P \sim 25\%$ - are undesirable. In such cases the (unsteady) wake of the (bluff) payload was wide and long enough, and the parachute internal pressure low enough, to cause a total collapse of the canopy during its steady state descent. Such an event was always followed by a rapid freefall and by re-inflation, which was then followed by another collapse and so on. Such a deflation/re-inflation cycle was observed to repeat many times during each flight. Obviously, such large apex venting generated too small of an internal parachute pressurization to keep the canopy bulged outwards when the parachute skirt interacted with atmospheric- or payload-generated gusts.

3.3 Inflation Properties

Typical riser load evolution profiles are shown in figures 3.4 -3.6. The inflation sequence featured in figure 3.7 shows that TCDs never adopt the intermediate and temporary bulb-shape that is so typical of inflating hemispherical-type canopies. The riser load graphs point to inflation (or filling) times that are of the order of 2 to 3 seconds for the weight and aircraft speed used here.

Non-dimensional filling times can be calculated readily, but using a different size parameter. This is because TCD inflation consists in the air filling the canopy mostly along the longitudinal axis, in contrast to hemispherical canopies which fill mostly transversely (i.e. in the direction of the skirt's diameter). It is suggested that the non-dimensional filling time corresponding to TCD inflation be computed from a size scale dictated by the cone height H instead of the skirt diameter, at least for cones characterized by $H/B > 1$:

$$n_{fill} = \frac{V_{stretch} t_{fill}}{H} \qquad (3.1)$$

Using a value of the line-stretch speed ($V_{stretch}$) of 110 ft/sec, the corresponding value of n_{fill} falls in the range of $n_{fill} \sim 13 - 20$. The value of $V_{stretch}$ used in this calculation was arrived at by using the PIMS parachute inflation simulation software, which estimates a payload container's fall speed prior to parachute deployment, while taking into account the aircraft speed at drop time together with the container's weight, size, shape and drag properties[6].

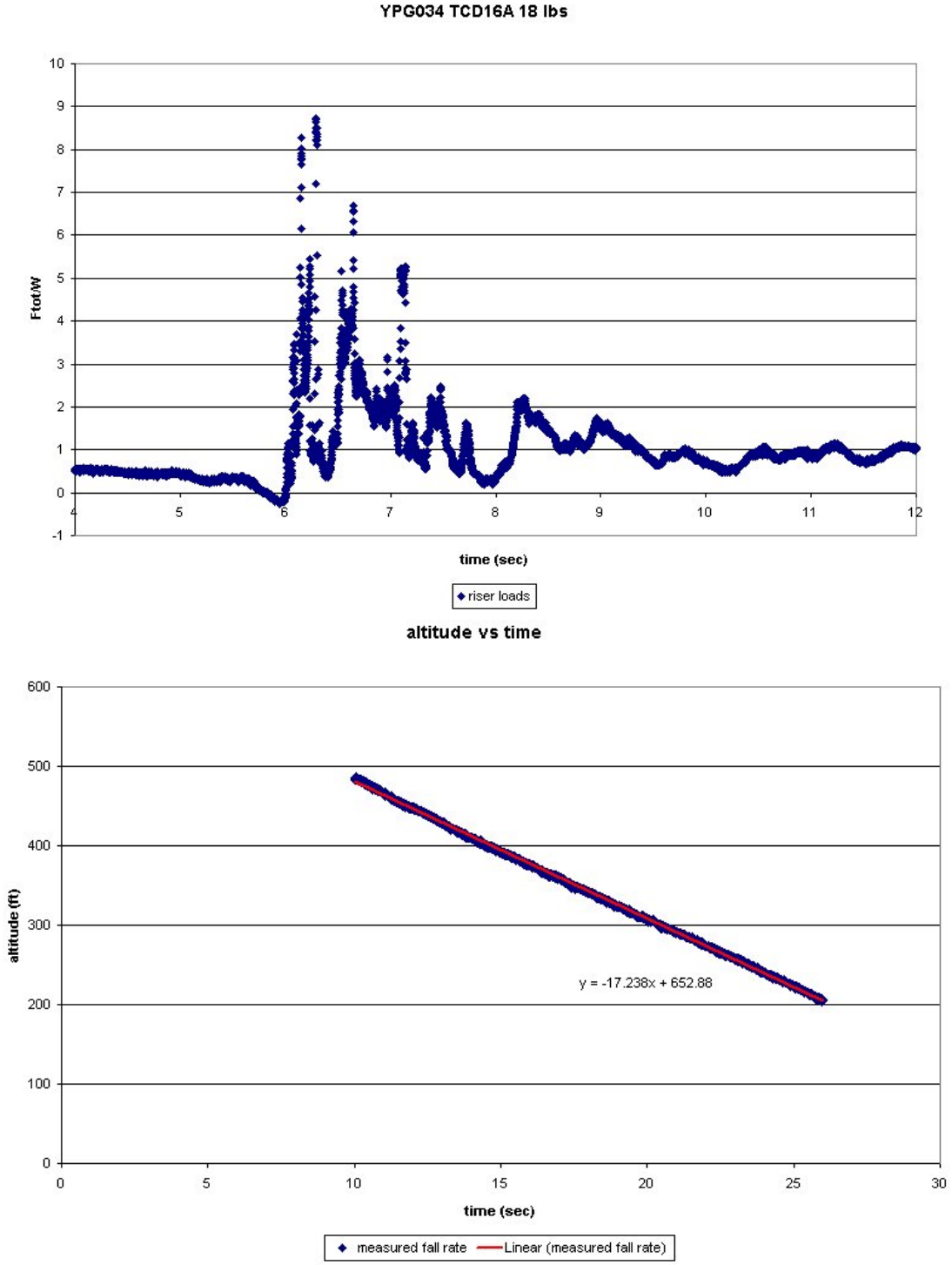

Figure 3.4 Riser loading and fall rate curves measured during drop YPG034. The lower figure also includes a linear fit to the data. The time on each curve is synchronized. The fall rate curve does not include inflation. Video confirms that inflation ends at $t \sim 10$ sec.

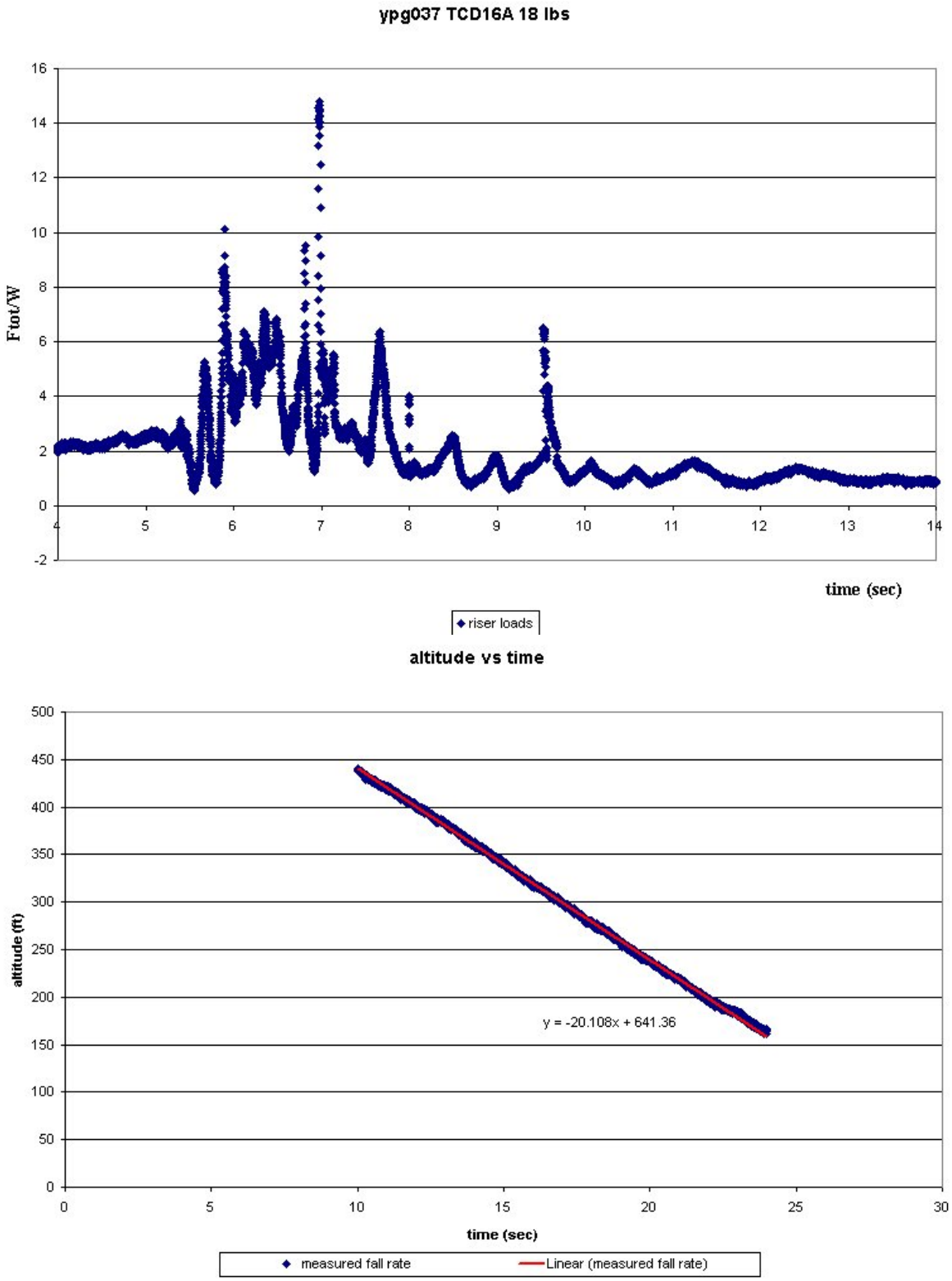

Figure 3.5 Riser loading and fall rate curves measured during drop YPG037. The lower figure also includes a linear fit to the data. The time on each curve is synchronized. The fall rate curve does not include inflation, Video confirms that inflation ends at *t* ~ 10 sec.

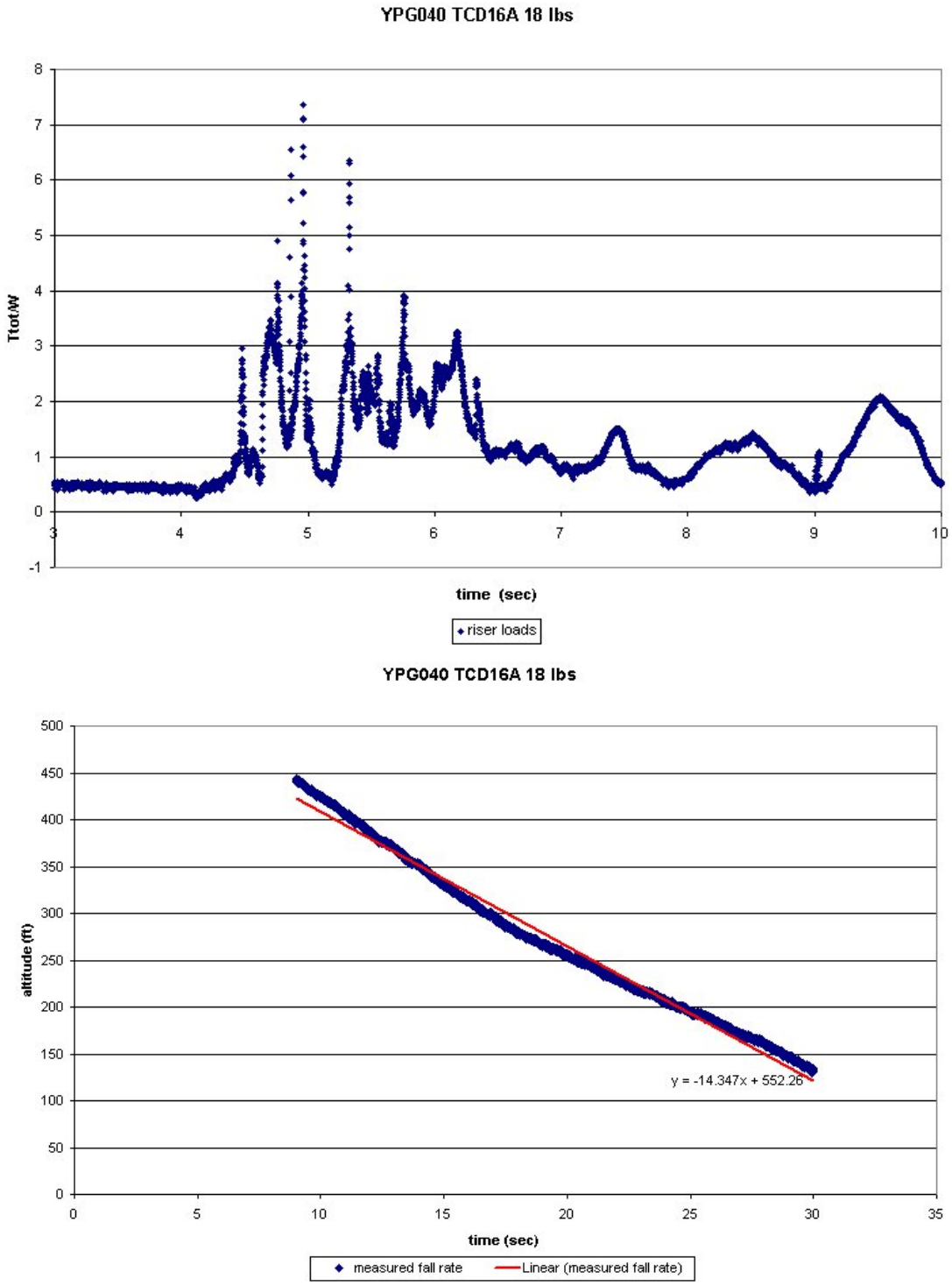

Figure 3.6 Riser loading and fall rate curves measured during drop YPG040. The lower figure also includes a linear fit to the data. The time on each curve is synchronized. The fall rate curve does not include inflation. Video confirms that inflation ends at *t* ~ 10 sec. Note that this data was measured during a windy and (somewhat) warm day, which lead turbulent conditions near the ground and to relative canopy-payload motions and (shallow) oscillations during the steady-state descent (namely after the 8 seconds-mark).

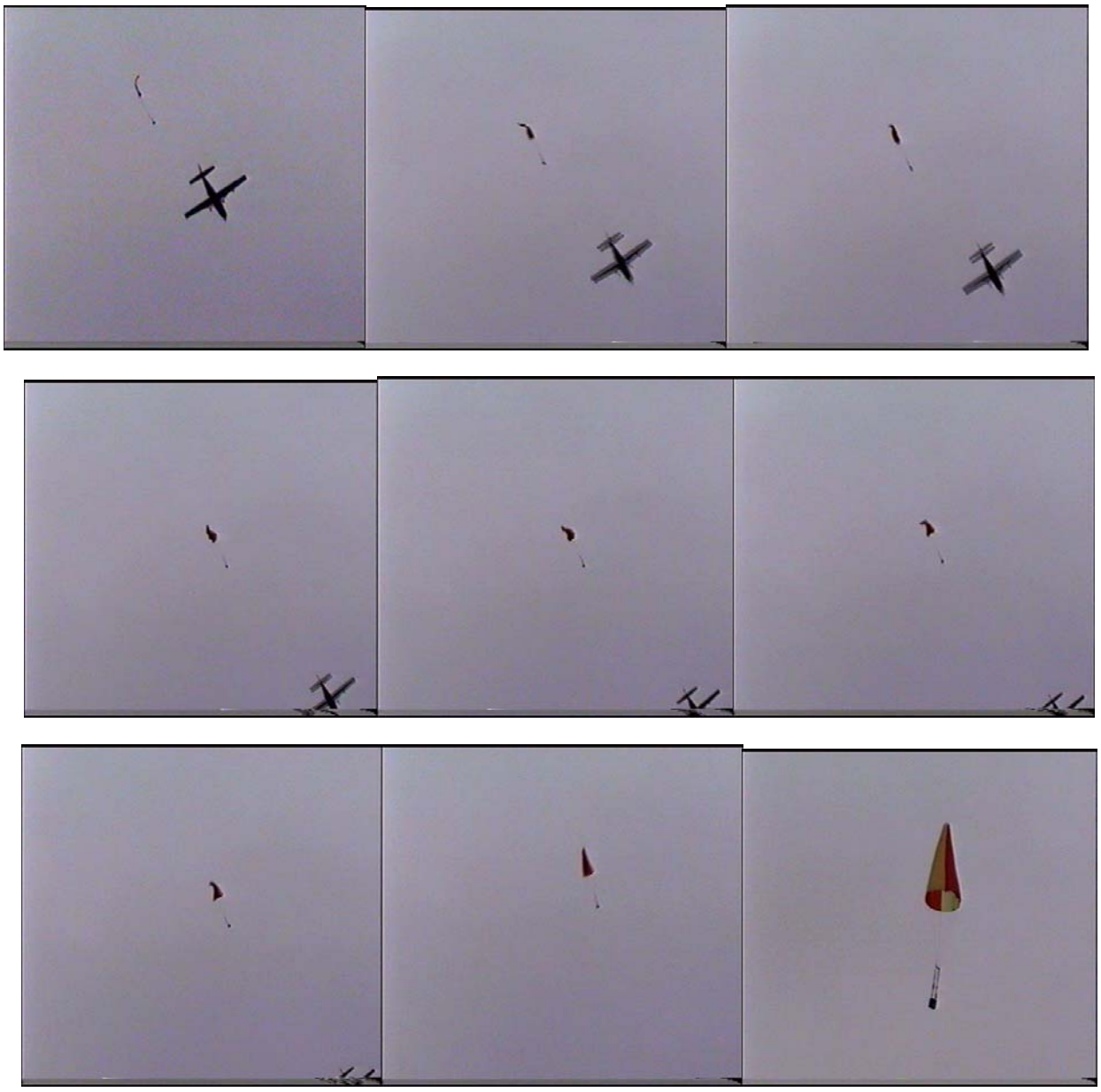

Figure 3.7 Inflation sequence of the 16ft TCD used during drop YPG034, as filmed from the ground

Two other important estimators for inflation analysis are the mass ratio R_m and opening shock factor C_k. The former is a rough measure of the ratio of a parachute-payload total weight, relative to that of the air co-accelerating or decelerating with the system [5,7]:

$$R_m = \frac{W_{total}}{g\rho\left(SC_D\Big|_{steady}\right)^{1.5}} \tag{3.2}$$

The C_k –factor expresses, in non-dimensional units, the maximum force sustained during inflation[5,7]:

$$C_k = \frac{2F_{\max}}{\rho(SC_D\big|_{steady})V^2_{stretch}} \tag{3.3}$$

Using the data collected with the full-scale parachute system, and in particular using the measured fall rate of $V_{steady} \sim 19\ ft/sec$, one obtains a drag area value of $SC_D\big|_{steady} \sim 45.3ft^2$. This value yields a mass ratio of $R_m \sim 0.83$ when used in (3.2). Such a R_m -value qualifies our full-scale TCD parachute-payload system as a low-mass ratio system. Note that this estimate has used $\rho \sim 0.0022$ sl/ft^3. On the other hand, looking at figures 3.4 – 3.6 suggests a maximum drag force approximating the 4g-mark, thus suggesting $F_{max} \sim 4W \sim 72lbs$, and yielding an opening shock factor of the order of $C_k \sim 0.12$. Such a C_k -value at $R_m^{-1} \sim 1.2$ is very typical of the unreefed or permanently-reefed hemispherical parachute systems that Wolf has analyzed in his C_k Vs. R_m^{-1}plot. See reference 7 for details.

4. Concluding Remarks

The shape of the TCD is novel enough to warrant more studies of its behavior, during inflation as well as during the steady state descent. For example, it would be interesting to investigate in more details the Reynolds number (R_e) -dependence of the steady state drag coefficient, and see whether it is insensitive to R_e in the same manner that characterizes most round parachutes[5]. Given its extreme rearward streamlining, it would be interesting to see whether flow separation occurs near the skirt area as with round parachutes[5], or much farther down the cone – i.e. closer to the vent. If true this scenario would yield a much narrower wake. Another topic of interest could be the inflation modeling of conical parachutes. Given the fact that TCDs do not produce the characteristic (intermediate) bulb shape that is seen with so many hemispherical types, and given that full skirt expansion occurs *at the beginning* of inflation rather than at the end, it is doubtful that the models used to simulate inflation of hemispherical parachutes would work well when applied to the TCD. Clearly, some new modeling insight is needed. Finally, further studies should be carried out with TCDs of aspect ratios differing from the value of 2.3, in order to document drag and inflation property changes as a TCD evolves from the shape of a near-tube to that of a near-hemisphere.

Acknowledgments

The authors would like to thank the following individuals for their hard work while supporting the test drops of the full-scale TCD system: Mr. E. Brighton and Mr. M. Farmer, undergraduate students at Saint Louis University, and Mr. D. Cunningham and Mr. R. Holland (sub-contractors). We would like to thank also Mr. R. Wright from Planning Systems Inc., and Dr. R. Howard from the Yuma Testing Center for useful discussions. Portions of this work were performed under funding from the US Army Yuma Proving Ground (contract W9124R-04-P1272).

VHT (in) **VHT/H %** **(see figure 5)**	**VHT/H (%)** **S_V/S_P (%)** **S_V/S_T (%)** **S_T (ft^2)**	**Fall rate** **(ft/sec)** **± 2 ft/sec** **@ W = 4.1 lbs**	***Nominal drag coefficient*** ***C_{D0}***
0 0	0 0 0 17.93	32.6	0.19
4 6.3	6.3 .40 $8.4\ 10^{-2}$ 17.93	31.0	0.21
6 9.5	9.5 .90 $1.91\ 10^{-1}$ 17.93	26.9	0.27
8 12.6	12.6 1.6 $3.36\ 10^{-1}$ 17.93	27.8	0.26
10 15.9	15.8 2.5 $5.29\ 10^{-1}$ 17.93	27.5	0.26
12 19.0	19.0 3.61 $7.66\ 10^{-1}$ 17.93	29.5	0.23

Table 3.1 Fall rates measured on the sub-scale TCD. The values of the nominal drag coefficient are computed with the surface area S_T, which includes the area of the conical section that is removed to create a vent.

References

[1] Kelly, K., B. Pena; ;"Wind Study and GPS Dropsonde Applicability to Airdrop Testing"; AIAA-2001-2022; 16th AIAA Aerodynamic Decelerator Systems Technology Conference, Boston, MA 2001.
[2] Brocato, E; "Vertical Wind Analysis"; paper AIAA-2003-2163; *17th AIAA Aerodynamic Decelerator Systems Technology Conference and Seminar*, Monterey, CA, May 19 -22, 2003; pp. 430 – 437.
[3] J. Potvin, J. Papke, G. Peek, T. Hawthorne, E. Brighton and R. J. Benney; "Glide Performance Study of Standard and Hybrid Cruciform Parachutes"; paper AIAA-2003-2160; *17th AIAA Aerodynamic Decelerator Systems Technology Conference and Seminar*, Monterey, CA, May 19 -22, 2003; pp. 412 – 429.
[4] Philip D. Hattis, Thomas J. Fill, David S. Rubenstein, Robert P. Wright, and Richard J. Benney, "An Advanced On-Board Airdrop Planner to Facilitate Precision Payload Delivery," AIAA paper 2000-4307 presented at the AIAA Guidance, Navigation, and Control Conference, August 14-17, 2000, Denver, Colorado.
[5] T. W. Knacke, "Parachute Recovery Systems Design Manual"; Para Publishing (Santa Barbara, CA 1992).
[6] G. Peek, and J. Potvin; "PIMS – Parachute Inflation Modeling Suite – Version 2.1. The User's Manual"; May 14, 2004. Unpublished.
[7] Wolf, D., "Opening Shock", AIAA-99-1702, *15th CEAS/AIAA Aerodynamic Decelerator Systems Technology Conference and Seminar*, Toulouse, France, June 8-11, 1999.